ACTA MECHANICA SINICA, Vol.8, No.1, February 1992
Science Press, Beijing, China
Allerton Press, INC., New York, U.S.A.
ISSN 0567-7718

PSEUDO-MOLECULAR DYNAMICS STUDY OF GRAIN BOUNDARY SEGREGATION*

Zhou Fuxin (周富信)

(Lab for Non-Linear Mechanics of Continuous Media, Institute of Mechanics, Chineses Academy of Sciences, Beijing 100080, China)

Peng Bayi (彭八一) Wu Xijun (吴希俊) Tang Qiheng (汤奇恒)

(Institute of Solid State Physics, Chinese Academy of Sciences, Hefei 230031, China)

ABSTRACT: The segregation of bismuth atoms on the [101] tilt copper grain boundaries $\Sigma 3(\bar{1}\bar{1}1)$ 70.53°, $\Sigma 33(\bar{5}\bar{4}5)$ 58.99°, $\Sigma 11(\bar{3}\bar{2}3)$ 50.48° and $\Sigma 9(\bar{2}\bar{1}2)$ 38.94° has been studied by pseudo-molecular dynamics using the empirical N-body potentials. The relationship between bismuth segregation and grain boundary structure has been discussed in detail.

KEY WORDS: pseudo-molecular dynamics, empirical N-body potential, grain boundary segregation

I. INTRODUCTION

The grain boundary embrittlement (GBE) of metal copper caused by bismuth segregation has been extensively studied both experimentally and theoretically [1-14]. By using the orientation-controlled bicrystals, the strong dependence of Bi segregation upon grain boundary (GB) structures has been revealed[5,6]. The static study of Bi and Ag segregation on the [100] tilt GBs of copper and gold by Sutton and Vitek[9] showed that the segregation energy at various sites in a given GB differs widely and for a given structural unit, the segregation energy also varies considerably with its surrounding conditions in the GB. It was also found that the large Bi atoms go into those sites which are surrounded by a tensile stress field in the uncontaminated GB, that is, the segregation chooses the most spacious sites. It indicates that segregation is selective with respect to both GB type and the site in GB. Vitek et al.[10] studied the Bi segregation in some coincidence GBs of metal Cu. The results illustrated that the strong effect of the local atomic environment on the segregation energy leads to selectivity of segregation sites. As indicated by Balluffi, [24] impurity segregation is mainly confined to within a few atomic planes of GB. Computer simulation[12] also indicated that the impurity bismuth atoms tend to segregate in a few atomic layers in the copper GB. In our previous papers[14, 25] only a monolayer of Bi atoms segregated in the core of GBs was considered and the effect of selectivity of Bi segregation in GBs was not taken into account.

In this paper, Bi segregation for [101] tilt copper bicrystals $\Sigma 3(\bar{1}\bar{1}1)$70.53°, $\Sigma 33(\bar{5}\bar{4}5)$ 58.99°, $\Sigma 11(\bar{3}\bar{2}3)$50.48° and $\Sigma 9(\bar{2}\bar{1}2)$38.94° has been studied by pseudo-molecular dynamics using the empirical N-body potentials. The aim of this paper is to study the relationship between bismuth segregation and GB structure and to compare these results with those from Refs.[9,10].

II. INTERATOMIC POTENTIAL AND CALCULATION METHOD

2.1 Interatomic Potential

In recent years considerable efforts have been devoted to the study of atomistic models suitable for computer simulations of metallic systems[15, 16] in order to include many-body interactions, in the early pairwise potentials an accompanying volume-dependent energy needs to be used. [17] With his volume-dependent term, it is still difficult to simulate surfaces and to

Received 11 June 1991
* The subject supported by the Chinese Academy of Sciences and National Natural Science Foundation of China

consider crystal defects, where the volume of the sample is ambiguous. Moreover, the vacancy-formation energy is always the same as the cohesive energy in a pair potential model, which, in fact, is incorrect.

Daw and Baskes[16] proposed a method called the Embedded Atom Method (EAM) to overcome those kinds of limitations in pairwise potentials. This new method is based on the theory of density function. It uses the concept of quasiatom[18] or effective-medium[19] approach. In the EAM, the electron density of the sample is allowed to vary from one lattice site to another and the cohesion at a given lattice site depends on the local electron density at the site, which is approximated by the superposition of electron densities of the surrounding atoms. The total energy is divided into a pairwise interaction plus an embedding energy, which is the energy required to place an atom in a uniform electron gas. Empirical EAM functions for the fcc metals of Ag, Au, Cu, Ni, Pd and Pt, and their alloys were developed by Foiles, Baskes, and Daw[20] by numerically fitting the functions to the bulk lattice constants, cohesive energy, elastic constants, vacancy-formation energy and alloy mixing heat. These EAM functions have been fairly successful in a wide range of applications. [21]

Finnis and Sinclair[15] have independently developed a model which is mathematically equivalent to the EAM. According to their scheme, the energy of an atom i is written as the sum of a pairwise term acting between atoms i and j and a term which depends on the local atom density ρ_i :

$$u_i = -f(\rho_i) + 1/2\sum_j V_{ij} \tag{1}$$

where ρ_i is expressed as a sum of atomic functions

$$\rho_i = \sum_j \Phi_{ij} \tag{2}$$

V_{ij} and Φ_{ij} are functions only of the interatomic distance between i and j and are of short-range. A square root function is chosen for f. Using this scheme, N-body potentials for copper, silver, gold and nickel were constructed by Ackland et al.[22]

In the present work, we have constructed the empirical N-body potentials to describe the atomic interaction in the Cu-Bi binary system according to this scheme[15] and the EAM[16]. The functions $V(r)$ and $\Phi(r)$ for copper constructed by Ackland et al.[22] have been adopted to describe the interatomic potential for Cu-Cu atoms. In the construction of potential for bismuth, whose crystalline structure is trigonal, the lattice is approximated by a simple cubic structure with the same density.[23] The functions $V(r)$ and $\Phi(r)$ for bismuth are determined by fitting them to the lattice parameter, cohesive energy, the elastic constants and the vacancy-formation energy. The potential functions for pure copper and bismuth are used in the binary system because changes of the potential curves for Cu-Cu and Bi-Bi atoms due to the variation of Bi concentration are too small to be noticeable, as indicated by Maeda et al.[23] In order to describe the interaction between Cu-Bi atoms, the pairwise term $V(r)$ for Cu-Bi is derived by fitting it to the mixing enthalpy of the Cu-Bi alloy. Since available data of the Cu-Bi alloy are limited and the assumption of simple cubic lattice for bismuth is made in the potential construction, the empirical N-body potentials constructed here are not perfect.

2.2 Calculation Method

The segregation of Bi atoms in [101] symmetric tilt copper GBs $\Sigma 9(\bar{2}\,\bar{1}\,2)$ 38.9°, $\Sigma 11(\bar{3}\,\bar{2}\,3)$ 50.48°, $\Sigma 33(\bar{5}\,\bar{4}\,5)$ 58.99° and $\Sigma 3(\bar{1}\,\bar{1}\,1)$ 70.53° has been studied by pseudo-molecular dynamics.

The computational cell is chosen to be a bicrystal slab, similar to that in our previous work[14]. Periodic border conditions are used in the directions parallel to the GB plane. Along the tilt axis, two adjacent (202) planes are periodically repeated. In the other direction perpendicular to the tilt axis, the period of the cell is one CSL vector of the corresponding GB or its multiples, which is about 5a long (where a is the lattice constant of copper). In the direction

normal to the GB plane, a fixed border is employed.

The Bi segregation is simulated in the following steps. The relaxation structure of the pure GB is first simulated by pseudo-molecular dynamics under the pressure within ±10 atm. The repeated relaxations of the atomic configuration make the internal energy reach minimum. During the simulation, only local atomic relaxation is allowed while the rigid body translation of the two grains forming the bicrystal is not considered here. Then, a large number of possible substitutional segregation sites are tested within about 5 Å (1 Å $=1\times10^{-10}$m) from the GB plane due to the fact that the great majority of the segregated atoms generally lie in a narrow zone of GB within a few atomic layers from the centre plane of the GB[24]. A bismuth atom is then placed into a site with the lowest segregation energy. Afterwards, the configuration with impurity relaxes again by pseudo-molecular dynamics. [25] By placing another Bi atom successively into various possible segregation sites until the most favoured site for its segregation is again found. This process is repeated, increasing gradually the concentration of the impurity in the GB. When the energy change of the system induced by a Bi atom segregation in the GB exceeds that induced by replacing the Cu atom in the grain with certain bulk concentration C of Bi with a Bi atom, the segregated Bi concentration will be considered as reached at the bulk concentration C.

To interpret the segregation behaviour, the hydrostatic stress fields of the GBs are also calculated. The $\alpha\beta$ component of the stress tensor [9] of atom i is

$$\sigma_i^{\alpha\beta}=\frac{1}{2\Omega_i}\sum_{j\neq i}^{N}[f'(\rho_i)\Phi_{ij}'+f'(\rho_j)\Phi_{ij}'-V_{ij}']\,r_{ij}^{\alpha}\times r_{ij}^{\beta}/r_{ij} \tag{3}$$

where r_{ij}^{α} is the α component of the vector r_{ij} connecting atoms i and j, Ω_i is the local atomic volume determined by Sutton's approximation[9]. The hydrostatic pressure is then given by

$$P_i=\frac{1}{3}\sum_{\alpha=1}^{3}\sigma_i^{\alpha\alpha} \tag{4}$$

III. COMPUTATIONAL RESULTS

3.1 Relaxed Structure of the Pure GBs

In the previous paper[14], the structures of Σ3 and Σ33 GBs were studied. Their structures as well as those of Σ9 and Σ11 GBs are also calculated under pressure within ±10 atm., which are shown in Fig. 1 (a)—(d) by projecting the atomic positions onto the (101) plane. In the figures, triangles and crosses represent the atomic positions in two adjacent (202) planes. The corresponding hydrostatic stress fields are shown in Fig. 1 (a′), (c′) and (d′) where arrows and hooks represent the hydrostatic stress at sites of atoms on (101) and (202) planes, respectively. Arrows and hooks pointing to the right indicate compression while those pointing to the left indicate tension. The magnitude of the stress is proportional to the length of the arrows and hooks.

As shown in Fig. 1 (a), the Σ9 GB is composed of only one kind of repeated structural unit (SU), i. e. pentagonal bipyramid (PB) plus capped trigonal prism. A large tensile hydrostatic stress exists at vertexes of the PBs (as shown in Fig. 1 (a′)), which indicates that the local atomic arrangement is spacious. The stress field only extends a few atomic layers to the grains from the GB plane.

The relaxed structure of Σ3 GB is the same as that in our previous study[14]. It consists of one kind of SU, i. e. irregular octahedron (IO) (as shown in Fig. 1 (b)). Since the Σ3 GB is a coherent twin boundary, the stresses in the field are very small.

It is shown in Fig. 1 (c) and Fig. 1 (d) that the structures of the Σ33 and Σ11 GBs, in which misorientations are between those of Σ3 and Σ9 GBs, are composed of the SUs of Σ3 and Σ9 GBs. That is to say, Σ9 and Σ3 GBs are the two favoured boundaries delimiting the

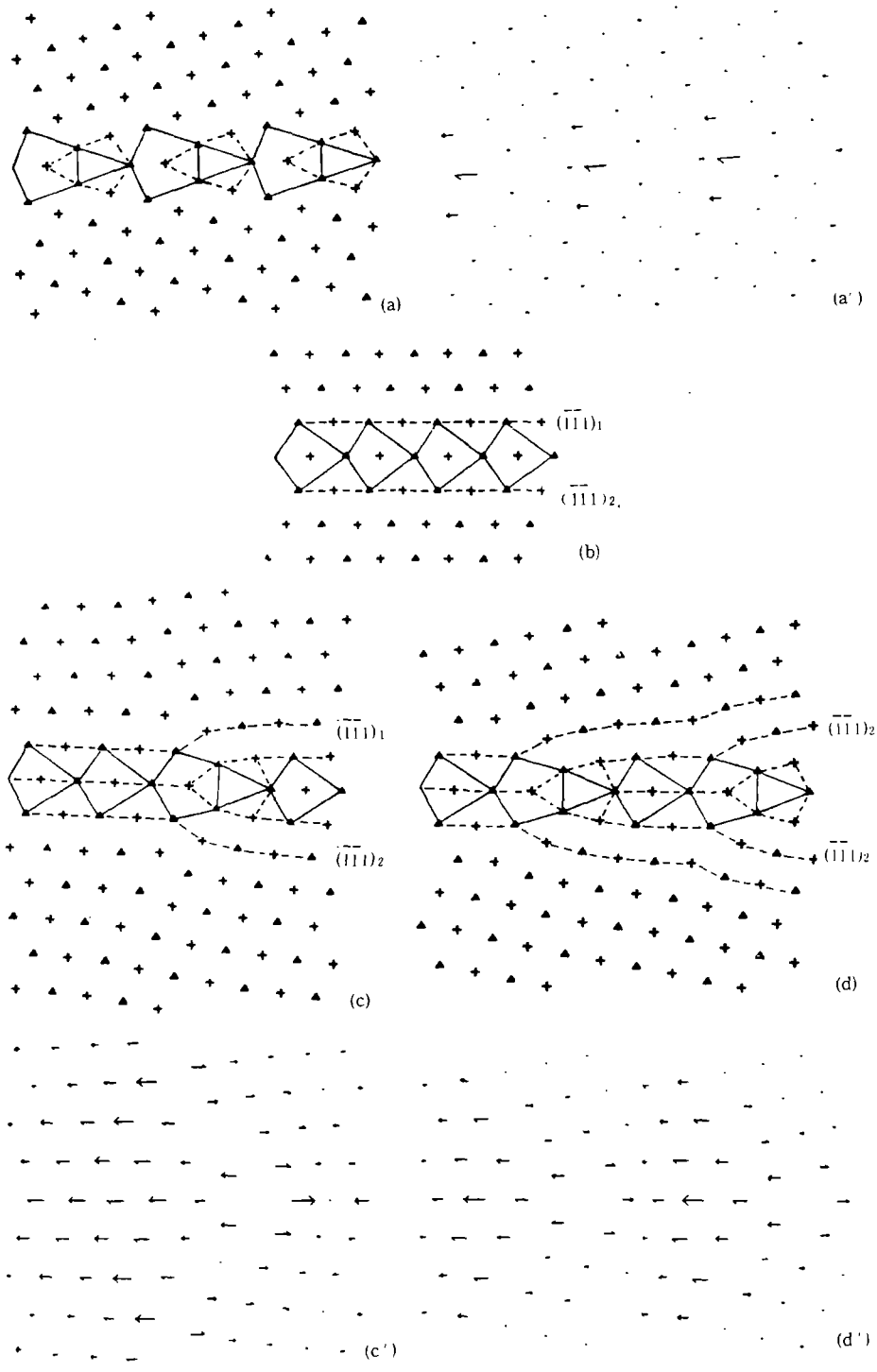

Fig. 1 The relaxed structures of the pure grain boundaries. (a) Σ9, (b) Σ3, (c) Σ33 and (d) Σ11; The corresponding hydrostatic stress of the grain boundaries (a′) Σ9, (c′) Σ33, and (d′)Σ11

misorientation in tetween 38.94 ° and 70.53°. The relaxed structure of Σ33 GB is made up of three SUs of Σ3 GB and one SU of Σ9 GB with an intrinsic GB dislocation (GBD) of $b=2/3[\bar{1}\bar{1}1]$ located at the Σ9 SU. The $(\bar{1}\bar{1}1)$ planes terminate at this unit. It is also confirmed by the stress field shown in Fig. 1(c′), which can be regarded as the superposition of that of Σ9 GB and that created by the array of uniform GBDs with spacing equal to $[\bar{2}\bar{5}2]$, that in the Σ9 SU the stress field changes from tension to compression. The stress field created by the array of GBDs extends much more widely than that of Σ9 GB.

As shown in Fig. 1 (d), the relaxed structure of Σ11 GB consists of equal number of Σ9 and Σ3 SUs. The array of intrinsic GBDs is located in the Σ9 SUs, with spacing $[\bar{1}\bar{3}1]$, as shown in Fig. 1(d′), which indicates that the stress changes from tension to compression in these units. The Burgers vectors are $b=2/3[\bar{1}\bar{1}1]$ with higher density than that in Σ33 GB. It can be seen that $(\bar{1}\bar{1}1]$ planes terminate at the Σ9 SUs. The stress field of Σ11 GB can also be considered as that of Σ9 GB superimposed with that of array of uniformly spacing GBD's. It is less extended into the grains than that of Σ33 GB. That is to say, the higher the density of array of GBDs (i. e. wall of GBDs) is, the less the stress field extends.

Table 1
The grain boundary energy

GB	Σ3	Σ33	Σ11	Σ9
GB energy (mJ/m^2)	24	834	1073	987

3.2 Bismuth Segregation in Σ9 GB

Figs. 2 (a) — (m) are the relaxed structures of Σ9 GB segregated by 1 to 13 Bi atoms, respectively, where the circles represent Bi atoms. It is shown that the most favourable sites for large Bi atom to segregate are the vertexes of PBs, see Figs. 2 (a)— (b). With the number of Bi atoms increasing, the trend changes. The 3rd—5th Bi atoms segregate at the corners of PBs instead of the vertexes, as shown in Figs.2 (c)— (e). As bismuth concentration further increases, the 10th-12th Bi atoms segregate at the vertexes of the original capping trigonal prism, as shown in Figs. 2(j)— (l). Bi segregation leads to GB migrating about a half atomic distance upper. The distribution of Bi atoms is of translational symmetry relative to the new GB plane. In the GB, the segregants form a layer-like structure parallel to the GB plane. Structure transformation is obviously observed. It is shown in Fig. 2(l) that after the segregation, the coordinates of the original vertexes of PB differ from those of uncontaminated GB. As bismuth atoms further increase, the 13th Bi atom substitutes the copper atom in the grain, as shown in Fig. 2 (m). Fig. 2 (j′) shows the hydrostatic stress map of Σ9 GB segregated by 10 Bi atoms. The segregation of the large Bi at oms induces local compression.

3.3 Bismuth Segregation in Σ11 GB

Figs. 3 (a)— (i) show the relaxed structure of Σ11 GB segregated by Bi atoms. The first Bi atom segregates at the corner of the PB (as shown in Fig. 3 (a)) instead of its vertex because of the existence of the intrinsic GBDs, while the second Bi atom segregates at the vertex of the PB (as shown in Fig. 3 (b)). Then, the 3rd Bi atom segregates at the corner of another PB (as shown in Fig. 3 (c)). The distributions of the Bi atoms in the two Σ11 CSLs within one computational cell are different owing to the Bi segregation sequence. The Bi atoms are distributed in the corresponding tensile region of the uncontaminated GB. The Σ3 SU, which is difficult to be segregated in the Σ3 GB, is also segregated by the 8th Bi atom here (as shown in Fig. 3 (g)) due to the local tensile stress field created by the intrinsic GBD. Bismuth segregation may also change the original stress field. The site in the uncontaminated GB, where the stress field contains a compression region, is segregated by the 9th Bi atom, as shown in Fig 3(h). No significant structure change occurs with the Bi segregation. The coordinates of the atoms in

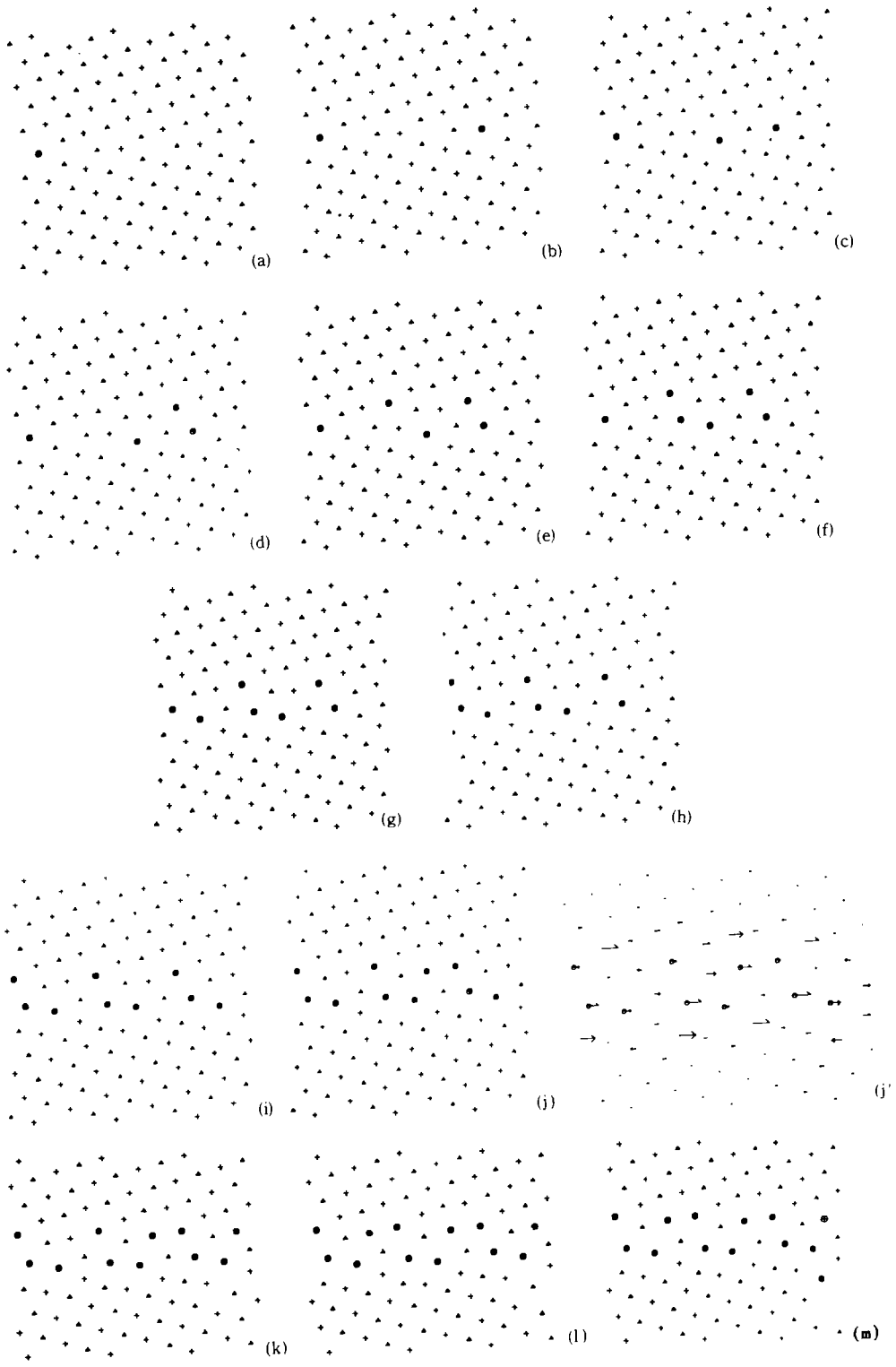

Fig. 2 (a)—(m) indicate the relaxed structure of the Σ9 grain boundary segregated by Bi atoms; (j') the hydrostatic stress of the grain boundary segregated by 10 Bi atoms.

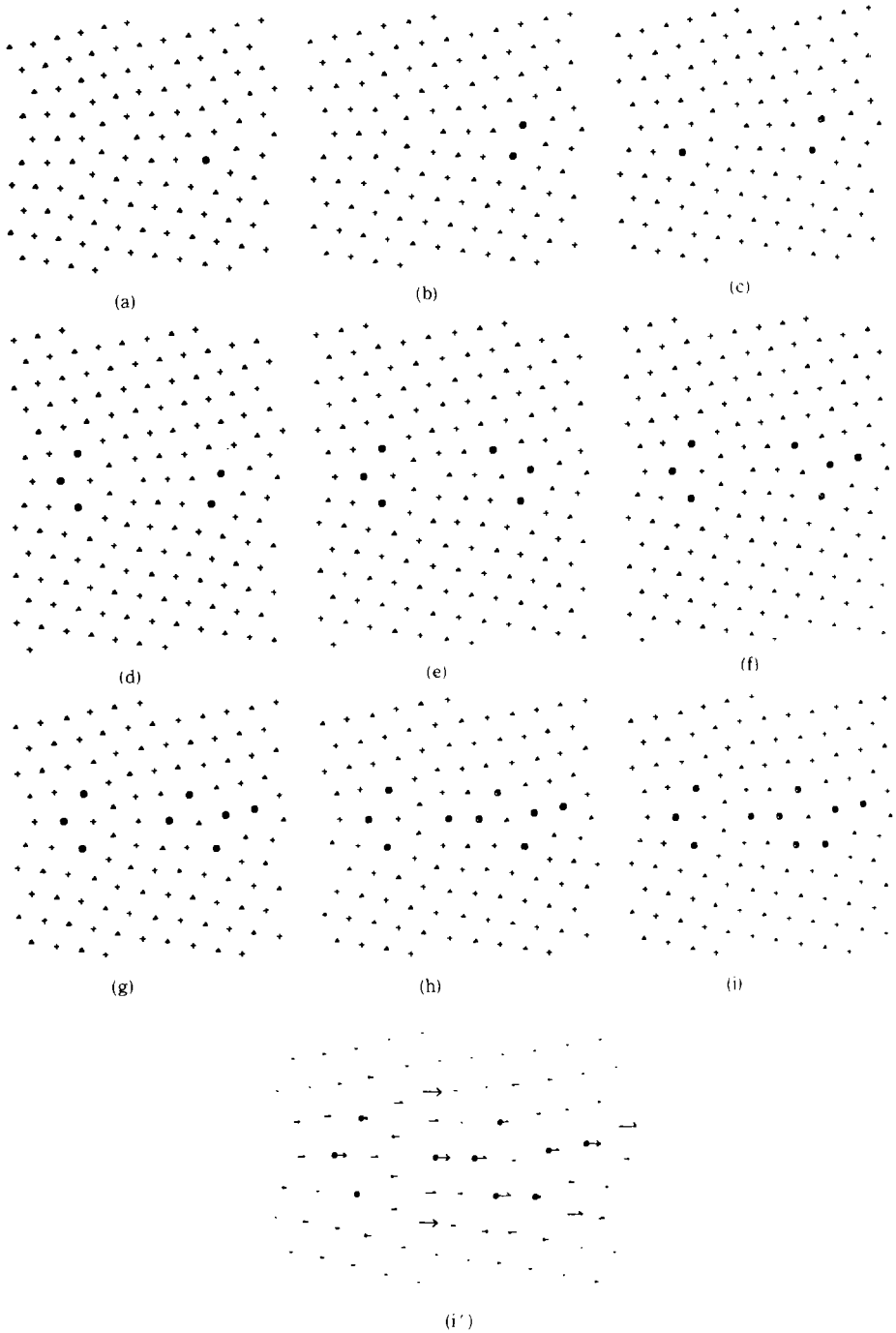

Fig. 3 (a)—(i) indicate the relaxed structure of the Σ11 grain boundary segregated by Bi atoms; (i′)the hydrostatic stress of the grain boundary segregated by 10 Bi atoms.

the GB core are similar to those in the pure GB core. Fig. 3(i′)is the hydrostatic stress field of the segregated GB with 10 Bi atoms. In contrast with Fig. 1 (c′), the bismuth segregation relaxes the stress field of the uncontaminated boundary.

3.4 Bismuth Segregation in Σ33 GB

The relaxed structure of the Σ33 GB segregated by Bi atoms is given in Fig. 4 (a) — (f). It is also observed that Bi segregation is affected by the presence of the intrinsic GBD and the most favourable site for segregation is the corner of the PB. The Bi atoms segregate in the tensile region of the stress field of the uncontaminated GB. The stress field is shown in Fig.4(f′). It is much more relaxed by the Bi segregation.

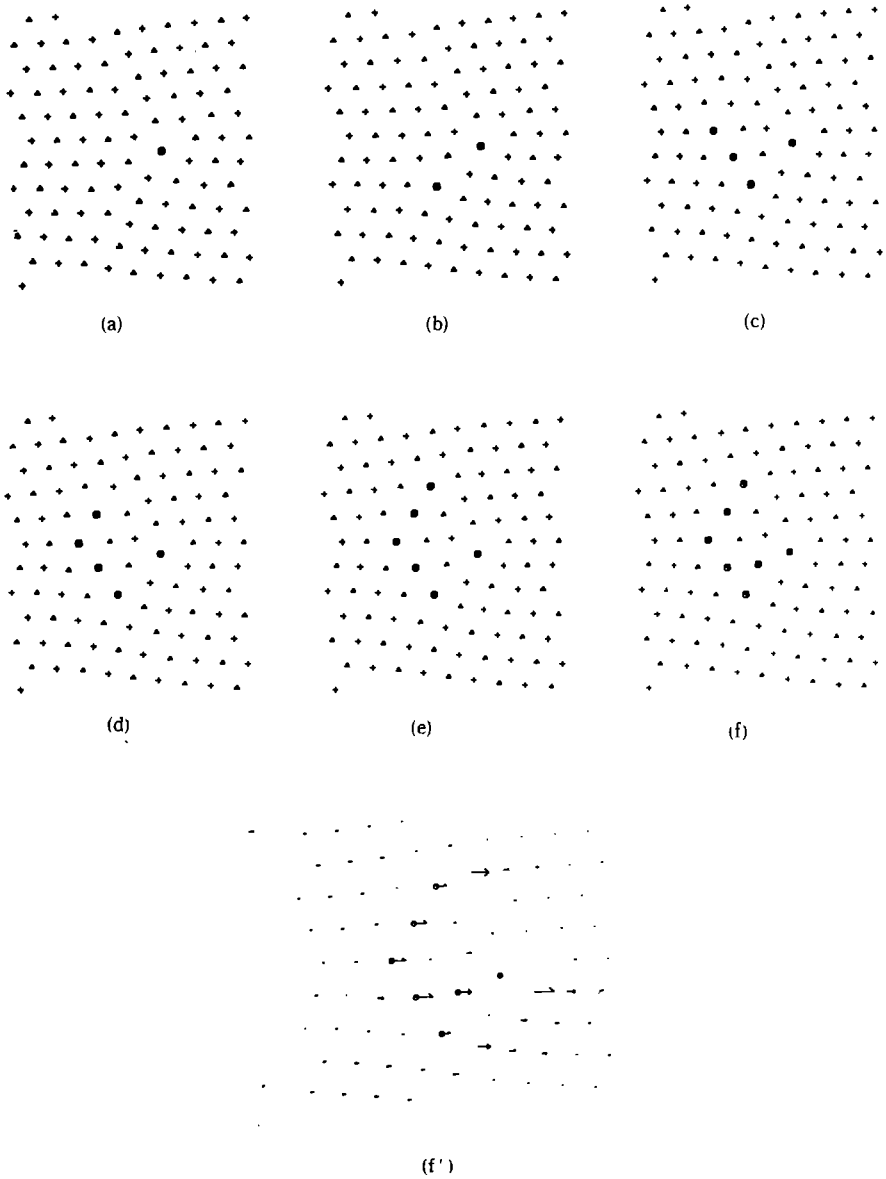

Fig. 4 (a)—(f) indicate the relaxed structure of the Σ33 grain boundary segregated by Bi atoms ; (f′) the hydrostatic stress of the grain boundary segregated by 7 Bi atoms

IV. DISCUSSION

The static study of Bi and Ag segregation in the [100] tilt GBs of copper and gold by Sutton and Vitek[9] showed that the segregation energy at various sites in a given GB differs widely and the segregation energy also varied considerably with its surrounding in the GB for a given structural unit. It was also found that the large Bi atoms go into those sites which are surrounded by a tensile stress field in the uncontaminated GB, that is, the segregation chooses the most spacious sites. It indicates that the segregation is selective with respect to both GB type and site in the GB.

Our simulation gives similar results. Quite anisotropic distribution of Bi atoms has been found in the Σ33 and Σ11 GBs. Due to the variation of the GB structures, the Bi segregations in the SU of Σ9 , Σ11 and Σ33 GBs are very different. Our calculation indicates that the Bi segregation is strongly dependent on the GB structure. On the one hand, it is related to polyhedra constructing the GB core. Bi atom is easier to segregate in the PB, where the local atomic arrangement is spacious, than in the IO. Thus, with the increase of the relative number of PBs in the GBs Σ33, Σ11 and Σ9, the segregated Bi concentrations increase in order. On the other hand, the GBD may affect the Bi segregation in the GB. Owing to the existence of the GBD, the IO, which is difficult to segregate in the Σ3 GB, is segregated by Bi atom in the Σ33 GB (see Fig. 4(c)) and the Σ9 SU exhibits different behaviour in the Σ9 , Σ11 and Σ33 GBs. The more widely the stress field of the GBD extends into the grains, the more dispersively the Bi atoms distribute, as can be seen in the Σ33 GB (see Fig. 1 (c′)) with respect to Σ11 and Σ9 GB (see Fig. 1 (d′) and Fig. 1 (a′)). Similar to Sutton and Vitek, the Bi atoms are found mainly to be distributed in the tensile region of the stress field of GB.

Additionally, the early segregation of Bi atoms may also affect the subsequent Bi segregation. The equivalent sites in the uncontaminated GB, e. g. the sites in the Σ9 GB (see Fig. 2 (a) and (f)) have different propensity for Bi segregation. And two equivalent Σ9 SUs in the uncontaminated Σ11 GB have different Bi distribution (see Fig. 3 (b) and (c)) because of the Bi segregation. These phenomena may be important in the actual dynamic process of Bi segregation. It may result in the reconstruction of the GB structure, such as GB migration and faceting.

It is also found that there is no obvious relation between the Bi segregation and the GB energy. As shown in Table 1, the Σ9 GB possesses lower GB energy than Σ11 GB, but shows higher capacity for Bi segregation. It may be due to the fact that the segregation is determined by the local structure of the GB core while the GB energy is determined by the whole lattice distortion induced by the GB which is affected by the long-ranged forces. Because the large tensile stress in the GB core is highly localized, the Σ9 GB is much easier to be segregated and has higher enrichment concentration of Bi atoms.

V. SUMMARY

Molecular dynamics can describe the microprocess of Bi segregation and the main results obtained illustrate the influence of GB structure upon Bi segregation.

(1) Bi segregation is related to the polyhedra which construct the GB core. The PB and, especially, its vertex is much easier to be segregated by the large Bi atom in the favoured GB Σ9, while the Bi atom is difficult to segregate in the IO which constructs the core of the favoured GB Σ3.

(2) Bi segregation is also influenced by the stress field of the array of GBDs. Due to the widely distributed stress field of GBDs in the Σ33 bicrystal, the Bi atoms distribute quite dispersively. The existence of the GBD might make the corner of the PB instead of its vertex the preferable site for Bi segregation and the IO, which is difficult to be segregated in the favoured Σ3 GB, is also segregated by the Bi atom in the Σ33 GB. Due to the structural dependence, the GBs Σ3, Σ33, Σ11 and Σ9 display increasing propensity for the bismuth segregation.

Additionally, the Bi segregation induces the structure transformation in the Σ9 GB

accompanying the GB migration, although it does not occur in the Σ33 and Σ11 GBs.

REFERENCES

1 Voce E, Hallowers A P C. J Inst Met, 1947, 73: 323
2 Joshi A, Stein D F. J Inst Met, 1971, 99: 178
3 Powell B D, Mykura H. Acta Metall, 1973, 21: 1151
4 Donald A M, Brown L M. Acta Metall, 1979, 27: 59
5 Fraczkiewicz A, Biscondi M. J Physique, 1985, 46: C4-497
6 Li G H, Wu X J, Cai M, Qin Q, Tang Q H. Scripta Metall., 1990, 24 (11): 2129
7 Dahl R E, Beeler J R, Bourquin R D. in: Gehlen P C, Beeler J R, Jaffee R I, ed. Interatomic potentials and simulation of lattice defects. New York: Plenum Press, 1972. 673
8 Nichols S. Scripta Metall, 1981, 15: 423
9 Sutton A P, Vitek V. Acta Metall, 1982, 30: 2011
10 Vitek V, Wang G J. Surf Sci, 1984, 144: 110
11 Hashimoto M, Ishida Y, Yamamots R, Doyama M. Acta Metall, 1984, 32:1
12 Chang H K, Lee J K, Stein D F. in: Lee J K, Ed. Interatomic potentials and crystalline defects. AIM, 1981. 373
13 Chang H K, Weidman R S, Lee J K. Surf Sci, 1984, 144: 224
14 Zhou F X, Peng B Y, Wu X J. J Appl Phys, 1990, 68 (2): 548
15 Finnis M W, Sinclair J E. Phil Mag, 1984, A50:45
16 Daw M S, Baskes M I. Phys Rev, 1984 B29: 6443
17 Johnson R A. Phys Rev, 1972 B6:2094
18 Stott M J, Zaremba E. Phys Rev, 1980, B22: 1564
19 NΦrskov J K. Phys Rev, 1982 B26: 2875
20 Foiles S M, Baskes M I, Daw M S. Phys Rev, 1986 B33: 7953
21 Foiles S M, Adams J B Phys Rev, 1989, B40:5909
22 Ackland G J, Tichy G, Vitek V, Finnis M W. Phil Mag, 1987, A 56: 735
23 Maeda K, Vitek V, Sutton A P. Acta Metall, 1982, 30: 2001
24 Balluffi R W. in: Johnson W D, Ed. Interfacial Segregation, AMS, 1979: 193
25 Zhou F X, Chen Z Y, Wu X J, Hu B, Acta Mech. Sinica, 1990, 22(1): 106 (in Chinese)